J|A|C|S
ARTICLES
Published on Web 04/23/2004

Spectroscopic Description of the Two Nitrosyl−Iron Complexes Responsible for Fur Inhibition by Nitric Oxide

Benoît D'Autréaux,[†] Olivier Horner,[†] Jean-Louis Oddou,[†] Claudine Jeandey,[†] Serge Gambarelli,[‡] Catherine Berthomieu,[§] Jean-Marc Latour,[†] and Isabelle Michaud-Soret*[,†]

Contribution from the Laboratoire de Physicochimie des Métaux en Biologie, UMR CNRS-CEA-UJF 5155, CEA-Grenoble, 38054 Grenoble Cedex 9, France; Service de chimie inorganique et biologique, FRE CEA-CNRS-UJF 2600, CEA-Grenoble, 38054 Grenoble Cedex 9, France; and Laboratoire de Bioénergétique Cellulaire, UMR 6191 CNRS-CEA-Université Aix-Marseille II, CEA-Cadarache, 13108 Saint-Paul-lez-Durance Cedex, France

Received December 12, 2003; E-mail: imichaud@cea.fr

Abstract: Ferric uptake regulation protein (Fur) is a global regulator, ubiquitous in Gram negative bacteria, that acts as a transcriptional repressor when it binds ferrous ion. Fur is involved in responses to several types of stress related to iron metabolism, such as stress induced by nitric oxide (NO) generated by macrophages against bacterial invasion. NO was recently shown to react with Fe^{2+} ions in FeFur (iron substituted Fur protein) leading to an Fur bound iron−nitrosyl complex, unable to bind DNA, and characterized by a $g = 2.03$ EPR signal, associated with an $S = {}^1/_2$ ground state. This electronic configuration could arise from either a mononitrosyl−iron $\{Fe(NO)\}^7$ or a dinitrosyl−iron $\{Fe(NO)_2\}^9$ complex. The use of several spectroscopic tools such as EPR, ENDOR, FTIR, Mössbauer, and UV−visible spectroscopies as well as mass spectrometry analysis was necessary to characterize the iron−nitrosyl species in Fur. Furthermore, changes of C132 and C137 into glycines by site directed mutagenesis reveal that neither of the two cysteines is required for the formation of the $g = 2.03$ signal. Altogether, we found that two species are responsible for Fur inhibition in NO stress conditions: the major species, $S_{1/2}$, is an $\{Fe(NO)_2\}^9$ ($S = {}^1/_2$) complex without bound thiolate and the minor species is probably a diamagnetic $\{Fe(NO)_2\}^8$ ($S = 0$) complex. This is the first characterization of these physiologically relevant species potentially linking iron metabolism and the response to NO toxicity in bacteria.

Introduction

Fur (ferric uptake regulation) is a global regulator ubiquitous in Gram negative bacteria, which controls the expression of more than 90 genes in *Escherichia coli*.[1] Fur is the key protein for the control of the intracellular iron concentration. The concentration of Fe^{2+} ions has to be tightly regulated in order to provide the needs of the cell and to prevent the Fenton reaction.[2] The Fur protein is a dimeric transcriptional repressor, activated by the coordination of one Fe^{2+} ion per monomer. The active form of the protein, FeFur (iron substituted Fur protein), binds to specific DNA sequences, called "iron boxes", located in the promoter region of genes involved in iron acquisition.[3] The binding of FeFur to the iron box hinders the access to DNA polymerase and leads to the repression of the downstream genes.[4] In contrast, when iron concentration is not sufficient, the active FeFur repressor releases the Fe^{2+} ions, Fur is no longer able to bind specific DNA sequences, and iron acquisition is then stimulated.

The Fur protein is thought to be involved in the defense against nitric oxide and makes a link between the control of iron homeostasis and response to NO stress.[5−7] NO is a cytotoxic weapon generated by macrophages that injures cells by attacking the iron centers in various key proteins such as ribonucleotide reductase[8] or ferredoxins.[9] Microorganisms have developed specific mechanisms which help to detoxify NO and to survive NO-mediated damages.[10−12] The synthesis of several enzymes

[†] Laboratoire de Physicochimie des Métaux en Biologie, UMR CNRS-CEA-UJF 5155.

[‡] Service de chimie inorganique et biologique, FRE CEA-CNRS-UJF 2600.

[§] Laboratoire de Bioénergétique Cellulaire, UMR 6191 CNRS-CEA-Université Aix-Marseille II.

(1) Hantke, K. *Curr. Opin. Microbiol.* **2001**, *4*, 172−177.
(2) Touati, D. *Arch. Biochem. Biophys.* **2000**, *373*, 1−6.
(3) de Lorenzo, V.; Giovannini, F.; Herrero, M.; Neilands, J. B. *J. Mol. Biol.* **1988**, *203*, 875−884.
(4) Escolar, L.; de Lorenzo, V.; Pérez-Martin, J. *Mol. Microbiol.* **1997**, *26*, 799−808.
(5) Crawford, M. J.; Goldberg, D. E. *J. Biol. Chem.* **1998**, *273*, 34028−34032.
(6) D'Autreaux, B.; Touati, D.; Bersch, B.; Latour, J. M.; Michaud-Soret, I. *Proc. Natl. Acad. Sci. U.S.A.* **2002**, *99*, 16619−16624.
(7) Mukhopadhyay, P.; Zheng, M.; Bedzyk, L. A.; LaRossa, R. A.; Storz, G. *Proc. Natl. Acad. Sci. U.S.A.* **2004**, *101*, 745−750.
(8) Lepoivre, M.; Flaman, J. M.; Henry, Y. *J. Biol. Chem.* **1992**, *267*, 22994−23000.
(9) Rogers, P. A.; Ding, H. *J. Biol. Chem.* **2001**, *276*, 30980−30986.
(10) Nunoshiba, T.; DeRojas-Walker, T.; Wisnok, J. S.; Tannenbaum, S. R.; Demple, B. *Proc. Natl. Acad. Sci. U.S.A.* **1993**, *90*, 9993−9997.
(11) Crawford, M. J.; Goldberg, D. E. *J. Biol. Chem.* **1998**, *273*, 12543−12547.
(12) Gardner, A. M.; Helmick, R. A.; Gardner, P. R. *J. Biol. Chem.* **2002**, *277*, 8172−8177.

is induced in response to NO, such as the flavohemoglobin (Hmp)[13] and the flavorubredoxin (FlRb),[12,14] two NO-detoxifying enzymes. NO also induces oxidative stress defense, such as MnSOD.[7,10] The transduction of the NO signal generally involves a transcriptional regulator which is activated or deactivated by NO. This is the case of SoxR for activation of the oxidative stress defenses in response to NO[15] or NorR for the control of FlRb expression.[16] The mechanisms of iron homeostasis recovery, after NO stress, are still poorly understood. Nevertheless, we found that NO is able to modulate Fur repressor activity in *E. coli*.[6] Furthermore, the recent study of the transcriptional profile in *E. coli*, using microarray analysis, has emphasized the role of Fur in the protection of the cell against nitrogen reactive species.[7] The inhibition of Fur DNA binding activity probably stimulates iron acquisition in order to favor the reconstitution of iron proteins damaged by NO. Furthermore, the expression of the *hmp* gene, coding for Hmp, is under Fur control in *Salmonella typhimurium*.[5] The derepression of *hmp* by Fur inhibition is thought to directly help to detoxify nitric oxide. All these biological processes are assumed to operate through the same proposed mechanism where NO reacts directly with the iron center in FeFur, the active form of the protein. The reaction leads to a stable protein containing a nitrosyl−iron species and unable to bind DNA. The spectroscopic argument for this proposal is the appearance of a $g = 2.03$ EPR signal, involving both iron and NO which can be observed in vivo in Fur overproducing cells treated by NO.[6] Nevertheless, the nature and the localization of this iron−nitrosyl species remain unclear, and this is the concern of the data presented here.

The iron center of *E. coli* Fur is a non-heme high spin Fe(II) ($S = 2$), with oxygen and nitrogen donor ligands.[17,18] The recent X-ray structure of the Fur protein from *Pseudomonas aeruginosa*, determined at 1.8 Å, with a zinc ion in the regulatory site, in place of iron, reveals that the metal is six-coordinated by two nitrogens from the imidazole groups of His-86 and His-124, one oxygen from the side chain of Glu-107 and two oxygens from the bidentate carboxylate of Asp-88, the sixth position being occupied by a water molecule.[19] The overall structure is pseudo-octahedral. Furthermore, EXAFS experiments with the iron containing protein are in agreement with this environment. Similar results had been obtained by EXAFS, Mössbauer and magnetization studies of the FeFur protein of *E. coli*, where the Fe(II) is six-coordinated by oxygen and nitrogen donor ligands, with the sixth ligand at a longer distance.[18] If we assume that NO will first displace the water molecule or one oxygen of the bidentate carboxylate to bind to iron, the nitrosyl−iron complex should be of the type $\{Fe(NO)\}^7$, according to the formalism of the Enemark−Feltham notation.[20] Several examples of $\{Fe(NO)\}^7$ complexes with a ligand environment that may be similar to FeFur have been reported in model compounds,[21] as well as in some iron proteins after reaction with NO, such as lipoxygenase,[22] isopenicillin *N*-synthase,[23] or protocatechuate 4,5-dioxygenase.[24] The ground state of these nitrosyl−iron complexes is $S = {}^3/_2$. By contrast, the paramagnetic center in FeFurNO (NO treated FeFur) is characterized by an $S = {}^1/_2$ ground state.[6]

Two distinct types of nitrosyl complexes with an $S = {}^1/_2$ ground state have been reported in the literature. The first one comprises mononitrosyl−iron complexes, $\{Fe(NO)\}^7$ which are usually five- or six-coordinated by strong field ligands, such as amine or heme nitrogens and sulfur in octahedral based geometry (Table 1). The second one is a dinitrosyl−iron entity $\{Fe(NO)_2\}^9$. In these compounds, iron is generally four- or five-coordinated (including NO) by nitrogen, oxygen, or sulfur donor atoms, in an overall tetrahedral geometry (Table 2). The two types of complexes possess distinct spectroscopic features (Table 1 and Table 2). Indeed, the $\{Fe(NO)\}^7$ ($S = 1/2$) complexes exhibit larger N(NO) hyperfine coupling and smaller ^{57}Fe hyperfine coupling than the $\{Fe(NO)_2\}^9$ ($S = 1/2$) complexes. This has been explained by their respective electronic structure. Recent Mössbauer studies and DFT calculations have established that the electronic structure of the $\{Fe(NO)\}^7$ ($S = {}^1/_2$) complexes is best described as a low spin Fe(II) coupled with a radical NO group Fe(II)($S = 0$)−NO$^\bullet$($S = 1/2$).[35,36] This description means that the spin density is mainly located on the NO nitrogen, and it is in very good agreement with the EPR, Mössbauer, and also IR data. The description of the electronic structure of the $\{Fe(NO)_2\}^9$ ($S = 1/2$) complexes is still a matter of discussion, and two oxidation states of the iron have been proposed, either d^7 Fe(+I)[48,49] or d^9 Fe(−I).[40,50] Nevertheless,

(13) Poole, R. K.; Anjum, M. F.; Membrillo-Hernandez, J.; Kim, S. O.; Hughes, M. N.; Stewart, V. *J. Bacteriol.* **1996**, *178*, 5487−5492.
(14) Gomes, C. M.; Giuffre, A.; Forte, E.; Vicente, J. B.; Saraiva, L. M.; Brunori, M.; Teixeira, M. *J. Biol. Chem.* **2002**, *277*, 25273−25276.
(15) Ding, H. G.; Demple, B. *Proc. Natl. Acad. Sci. U.S.A.* **2000**, *97*, 5146−5150.
(16) Hutchings, M. I.; Mandhana, N.; Spiro, S. *J. Bacteriol.* **2002**, *184*, 4640−4643.
(17) Adrait, A.; Jacquamet, L.; Le Pape, L.; Gonzalez de Peredo, A.; Aberdam, D.; Hazemann, J. L.; Latour, J. M.; Michaud-Soret, I. *Biochemistry* **1999**, *38*, 6248−6260.
(18) Jacquamet, L.; Dole, F.; Jeandey, C.; Oddou, J. L.; Perret, E.; Le Pape, L.; Aberdam, D.; Hazemann, J. L.; Michaud-Soret, I.; Latour, J. M. *J. Am. Chem. Soc.* **2000**, *122*, 394−395.
(19) Pohl, E.; Haller, J. C.; Mijovilovich, A.; Meyer-Klaucke, W.; Garman, E.; Vasil, M. L. *Mol. Microbiol.* **2003**, *47*, 903−915.
(20) Enemark, J. H.; Feltham, R. D. *Coord. Chem. Rev.* **1974**, *13*, 339−406.
(21) Schneppensieper, T.; Finkler, S.; Czap, A.; van Eldik, R.; Heus, M.; Nieuwenhuizen, P.; Wreesmann, C.; Abma, W. *Eur. J. Inorg. Chem.* **2001**, 491−501.
(22) Salerno, J. C.; Siedow, J. N. *Biochim. Biophys. Acta* **1979**, *579*, 246−251.
(23) Chen, V. J.; Orville, A. M.; Harpel, M. R.; Frolik, C. A.; Surerus, K. K.; Munck, E.; Lipscomb, J. D. *J. Biol. Chem.* **1989**, *264*, 21677−21681.
(24) Arciero, D. M.; Lipscomb, J. D.; Huynh, B. H.; Kent, T. A.; Munck, E. *J. Biol. Chem.* **1983**, *258*, 14981−14991.
(25) Liu, M. C.; Huynh, B. H.; Payne, W. J.; Peck, H. D., Jr.; Dervartanian, D. V.; Legall, J. *Eur. J. Biochem.* **1987**, *169*, 253−258.
(26) Liu, M. C.; Liu, M. Y.; Payne, W. J.; Peck, H. D., Jr.; Le Gall, J.; DerVartanian, D. V. *FEBS Lett.* **1987**, *218*, 227−230.
(27) Wayland, B. B.; Olson, L. W. *J. Am. Chem. Soc.* **1974**, *96*, 6037−6041.
(28) Nasri, H.; Ellison, M. K.; Chen, S.; Huynh, B. H.; Scheidt, W. R. *J. Am. Chem. Soc.* **1997**, *119*, 6274−6283.
(29) Franz, K. J.; Lippard, S. J. *J. Am. Chem. Soc.* **1999**, *121*, 10504−10512.
(30) McDonald, C. C.; Phillips, W. D.; Mower, H. F. *J. Am. Chem. Soc.* **1965**, *87*, 3319−3326.
(31) Danon, J. *J. Chem. Phys.* **1963**, *39*, 236−237.
(32) Feltham, R. D.; Enemark, J. H. *Top. Stereochem.* **1981**, *12*, 155−215.
(33) Hauser, C.; Glaser, T.; Bill, E.; Weyhermueller, T.; Wieghardt, K. *J. Am. Chem. Soc.* **2000**, *122*, 4352−4365.
(34) Sellmann, D.; Blum, N.; Heinemann, F. W.; Hess, B. A. *Chem.−Eur. J.* **2001**, *7*, 1874−1880.
(35) Li, M.; Bonnet, D.; Bill, E.; Neese, F.; Weyhermueller, T.; Blum, N.; Sellmann, D.; Wieghardt, K. *Inorg. Chem.* **2002**, *41*, 3444−3456.
(36) Pitarch Lopez, J.; Heinemann, F. W.; Prakash, R.; Hess, B. A.; Horner, O.; Jeandey, C.; Oddou, J.-L.; Latour, J.-M.; Grohmann, A. *Chem.−Eur. J.* **2002**, *8*, 5709−5722.
(37) Butler, A. R.; Glidewell, C.; Hyde, A. R.; Walton, J. C. *Polyhedron* **1985**, *4*, 797−809.
(38) Strasdeit, H.; Krebs, B.; Henkel, G. *Z. Naturforsch., B: Chem. Sci.* **1986**, *41B*, 1357−1362.
(39) Crow, J. P.; Cullen, W. R. *Can. J. Chem.* **1971**, *49*, 2948−2952.
(40) Bryar, T. R.; Eaton, D. R. *Can. J. Chem.* **1992**, *70*, 1917−1926.
(41) Li, L.; Morton, J. R.; Preston, K. F. *Magn. Reson. Chem.* **1995**, *33*, S14−S19.
(42) Basosi, R.; Laschi, F.; Rossi, C. *J. Chem. Soc., Perkin Trans. 2* **1978**, 875−880.
(43) Reginato, N.; McCrory, C. T.; Pervtsky, D.; Li, L. *J. Am. Chem. Soc.* **1999**, *121*, 10217−10218.

Table 1. EPR, Mössbauer, and IR Parameters of Selected $\{Fe(NO)\}^7$, $S = {}^1/_2$ Complexes

	CN[a]	$A(^{14}N_{NO})$[b]	$\delta_{/Fe}$[c]	ΔE_Q[c]	$A_{iso}(^{57}Fe)$[e]	ν(NO)[f]	ref
*cd*1 NIR	6	−; 44; −	0.34	+0.8	−8.3		25, 26
[Fe(TPP) (NO)]	5	35.3; 48.1; 48.7	0.35	+1.24	−10	1678	27, 28
[Fe(TC-5,5)(NO)]	5		0.06[d]	+1.39[d]		1710	29
$[Fe(DMTC)_2(NO)]$	5	35.3; 34.2; 41.7	0.46[d]	+0.81[d]		1724	30−32
trans-$[Fe(cyclam)(Cl)(NO)]^+$	6	327.6; 148.4; 179.2	0.27	+1.26	−11.6	1620	33
$[Fe(pyS_4)(NO)]$	6	33; 40; 20	0.33	−0.40	−5.6	1670	34, 35
$[Fe(pyN_4)(NO)]^{2+}$	6	−; 64; −	0.31	+0.84		1620	36

[a] CN = coordination number. [b]Principal values of hyperfine tensor in MHz. [c]Isomer shift value ($mm{\cdot}s^{-1}$) at 4.2 K and quadrupole splitting value ($mm{\cdot}s^{-1}$) at 4.2 K, except [d]77 K. [e]Isotropic values of the ^{57}Fe hyperfine tensor in MHz, determined by EPR. [f]NO stretching frequencies in cm^{-1}. TPP = tetraphenylporphinato; TC = tropocoronand; DMTC = dimethyldithiocarbamate; cyclam = 1,4,8,11-tetraazacyclotetradecane; pyS_4 = 2,6-bis(2-mercaptophenylthiomethyl)pyridine; PyN_4 = 2,6-bis(1,1-methylamine-ethyl)pyridine.

Table 2. EPR, Mössbauer, and IR Parameters of Selected $\{Fe(NO)_2\}^9$, $S = {}^1/_2$ Complexes

	CN[a]	$A_{iso}(^{14}N_{NO})$[b]	$\delta_{/Fe}$[c]	ΔE_Q[c]	$A_{iso}(^{57}Fe)$[b]	ν(NO)[f]	ref
$[Fe(SPh)_2(NO)_2]^-$	4	6.7	0.08[d]	0.78[d]		1744, 1709	37, 38
$[Fe(Br)(PPh_3)(NO)_2]$	4		0.24[e]	1.02[e]		1790, 1734	39
$Fe(PO_4)(NO)_2$	4				36.1		30
$[Fe(CO)_2(NO)_2]^+$	4	9			42.3	1785, 1756	40, 41
$[Fe(MeIm)_2(NO)_2]^+$	4	10.1				1804, 1740	42, 43
[Fe(di-2-pyridyl ketone)$(NO)_2]^+$	4		0.38	0.66		1715, 1685	44
$Fe(proline)_2(NO)_2$	4	9.8			43.7		45
[Fe(8-quinolinolate)$(NO)_2$]	4	6.2	0.47	0.88		1758, 1685	46
[Fe(6-Me_3-TPA)$(NO)_2]^+$	5	*g*				1801, 1762	47

[a] CN = coordination number. [b]Isotropic values of the hyperfine tensor in MHz, determined by EPR spectroscopy. [c]Isomer shift value ($mm{\cdot}s^{-1}$) at 4.2 K and quadrupole splitting value ($mm{\cdot}s^{-1}$) at 4.2 K, except [d]296 K, [e]77 K. [f]NO stretching frequencies in cm^{-1}. [g]No hyperfine structure in the EPR spectrum recorded at 5 K. 6-Me-3-TPA = tris(6-methyl-2-pyridylmethyl)amine.

although a unified picture is still missing, all authors agree that the spin density is mainly localized on the iron ion. In addition, IR data reveal two different NO stretching frequencies, indicating that the two NO groups are not equivalent.

The structural description of the NO modified FeFur protein is essential to understand how the FeFur protein is able to sense NO and how inhibition occurs. For this purpose, we performed extensive spectroscopic studies using EPR, ENDOR, Mössbauer, UV−visible, and FTIR. The properties of FeFurNO were compared with model compounds and other NO modified proteins of the $\{Fe(NO)\}^7$ ($S = 1/2$) and $\{Fe(NO)_2\}^9$ ($S = 1/2$) families to discriminate between the two possible electronic structures. The number of NO bound to iron has been quantified by mass spectrometry analysis and by determination of the stoichiometry of the reaction. Identification of the other ligands of the iron has been attempted in order to localize the nitrosyl−iron center in the protein. The environment of the nitrosyl−iron center has been probed by ENDOR spectroscopy. Bis-thiolato-dinitrosyl−iron complexes show EPR and UV−visible spectral features that are similar to the FeFurNO species raising the possibility that NO releases the iron from the regulatory site and forms a dinitrosyl−iron cysteine complex at a separate site in Fur. *E. coli* Fur contains four cysteines (C92, C95, C132, and C137); two of them, C92 and C95, are known to be bound to the structural zinc site,[51,52] and the two others, C132 and C137, are reduced and easily accessible to alkylating agents.[52] The possibility that cysteines C132 and C137 are iron ligands in the nitrosyl−iron species has been investigated by site directed mutagenesis experiments.

Experimental Section

Chemicals and Biochemicals. Mohr's salt $Fe(SO_4)_2(NH_4)_2{\cdot}6\ H_2O$, diethylamine, BTP, EDTA, horse heart myoglobin, NO gas (98,5% purity), and NO gas enriched in ^{15}N (98% atom) were provided by Sigma-Aldrich Chemicals. Mohr's salt enriched in ^{57}Fe (97.5% atom) was from Chemgas and DEANO from Cayman Chemical. DEANO solutions were prepared in 10 mM NaOH. The DEANO/NO stoichiometry is 1.5 NO molecules for 1 DEANO molecule.[53] The dNTP were provided by Fermentas, the *Pfu* Turbo and *Dpn* I were provided by Stratagene, and *Eae* I was provided by Amersham Biosciences.

Site-Directed Mutagenesis. Two Fur mutants were made: a single variant, C132G, and a double variant, C132G, C137G. Site-directed mutagenesis was performed by polymerase chain reaction (PCR), using the pFur1 plasmid[6] as a template. Mutagenic primers were

(5′-GTGCCGAAGGCGAT*G*GCCGCGAAGATGAAC) for the single variant C132G and (5′-CTTTACGGTCAC*G*GTGCCGAAGGCGAT*G*-GCCGCGAAGATG) for the double variant (C132G, C137G). All constructs were sequenced commercially on both strands (Genome Express) over their entire length to ensure that only the desired mutations were introduced.

Purification of the apo-Fur and Preparation of FeFur. The *E. coli* Fur protein and its variants were overproduced in *E. coli* and purified to homogeneity according to published procedures.[6,17] To prepare ^{15}N enriched Fur protein, the following modifications were added to the previous procedure. The culture medium was a minimal medium, composed of ^{15}N enriched NH_4Cl (1 g/L), glucose (2 g/L), $MnCl_2$ (0.1 mM), $ZnSO_4$ (0.05 mM), $FeCl_3$ (0.05 mM), and a vitamins

(44) Dessy, R. E.; Charkoudian, J. C.; Rheingold, A. L. *J. Am. Chem. Soc.* **1972**, *94*, 738−745.
(45) Woolum, J. C.; Tiezzi, E.; Commoner, B. *Biochim. Biophys. Acta* **1968**, *160*, 311−320.
(46) Miki, E.; Motonaga, M.; Mizumachi, K.; Ishimori, T.; Katada, M. *Bull. Chem. Soc. Jpn.* **1982**, *55*, 2858−2862.
(47) Jo, D. H.; Chiou, Y. M.; Que, L. *Inorg. Chem.* **2001**, *40*, 3181−3190.
(48) Burlamacchi, L.; Martini, G.; Tiezzi, E. *Inorg. Chem.* **1969**, *8*, 2021−2025.
(49) Basosi, R.; Burlamacchi, L.; Martini, G.; Tiezzi, E. *J. Chim. Phys. Phys.-Chim. Biol.* **1975**, *72*, 89−91.
(50) Connelly, N. G.; Gardner, C. *J. Chem. Soc., Dalton Trans.* **1976**, 1525−1527.
(51) Jacquamet, L.; Aberdam, D.; Adrait, A.; Hazemann, J. L.; Latour, J. M.; Michaud-Soret, I. *Biochemistry* **1998**, *37*, 2564−2571.
(52) Gonzalez de Peredo, A.; Saint-Pierre, C.; Adrait, A.; Jacquamet, L.; Latour, J. M.; Forest, E.; Michaud-Soret, I. *Biochemistry* **1999**, *38*, 8582−8589.
(53) Maragos, C. M.; Morley, D.; Wink, D. A.; Dunams, T. M.; Saavedra, J. E.; Hoffman, A.; Bove, A. A.; Isaac, L.; Hrabie, J. A.; Keefer, L. K. *J. Med. Chem.* **1991**, *34*, 3242−3247.

mix.[54] Overproduction was induced with IPTG (0.5 mM), when the optical density at 600 nm reached the value of 0.5.

Protein concentrations were determined spectrophotometrically using an absorption coefficient at 277 nm of 0.4 mg^{-1} mL cm^{-1} per monomer of pure apo-Fur. Unless otherwise indicated, the samples of *E. coli* Fur protein used in this work were prepared in 100 mM BisTris propane (BTP) buffer at pH = 7.5, containing 100 mM KCl and deaerated by purging under a vacuum/argon line. Further equilibration with an anaerobic atmosphere was performed by incubation overnight in a glovebox at 5 °C, under gentle stirring. The incorporation of Fe^{2+} (0.95 equiv) was performed under anaerobic conditions as previously described.[18]

Titration of NO in DEANO Solutions. The concentration of NO resulting from the decomposition of DEANO was determined by a procedure based on conversion of deoxymyoglobin (deoxyMb) to nitrosyl myoglobin (MbNO).[55] The detail of MbNO concentration determination can be found in the Supporting Information. The MbNO concentration was plotted versus the DEANO volume added. The graph showed that MbNO concentration increases linearly with the total volume of DEANO added and reaches a maximum when all deoxyMb had reacted. The equivalent volume, V_{eq}, was determined at the intersection of two extrapolated lines corresponding to the linear increase and the plateau value, respectively. The concentration of NO, $[NO]_i$, was calculated as follows: $[NO]_i = V_{total} \times [deoxyMb]_0/V_{eq}$.

With the values $V_{total} = 250\ \mu L$, $[deoxyMb]_0 = 1.10(2)$ mM, and $V_{eq} = 5.2(1)\ \mu L$, we have determined $[NO]_i = 53(2)$ mM, corresponding to a DEANO concentration of 35(2) mM, which was very close to the concentration estimated from weight.

NO Reaction with FeFur. NO derivatives were prepared under anaerobic conditions using the NO generator, DEANO, or NO gas. For ENDOR, Mössbauer, FTIR, electronic absorption spectroscopies, and mass spectrometry, the samples were prepared by a general method, previously described,[6] and details of protein and DEANO concentrations are reported in the figure caption for each experiment. Two iron containing species were obtained after reaction with NO, $S_{1/2}$ and S_0 (see results), which ratio depends on the time of incubation of the apo-protein (before reconstitution with iron and reaction with NO). To obtain a larger amount of S_0, the incubation of the apo-protein was reduced from one night to 3 h. The stoichiometry of the reaction was determined by measuring the concentration of nitrosyl−iron species formed by adding a known amount of NO to FeFur. An FeFur solution ([Fur] = 1.80(1) mM; [FeFur] = 1.70(1) mM; $V = 500\ \mu L$) was exposed to a freshly titrated DEANO solution (35(2) mM, 6 × 15 μL) in six successive additions. Each addition was followed by 1 h 30 min of incubation at 20 °C. Then a 20 μL aliquot was taken and diluted with 180 μL of the protein buffer. A UV−visible spectrum was recorded, and the sample was transferred to an EPR tube and frozen for EPR measurements. For the determination of the NO concentration in the reaction mixture, according to the DEANO volume added, we took into account the previously removed volumes used for EPR and UV−visible measurements. The concentration of free NO in the reaction mixture was determined by titration with deoxyMb. For these measurements, a 2 μL aliquot was taken from the reaction mixture and mixed with 20 μL of a freshly prepared deoxyMb solution at 200 μM in 100 mM BTP buffer, pH = 7. After 2 h of reaction, UV−visible spectra were recorded with 20 μL of the reaction mixture, diluted in 820 μL of the protein buffer. The MbNO concentration was determined as described in the previous paragraph.

EPR Spectroscopy. X-band EPR spectra were recorded on a Varian E109 spectrometer equipped with an ESR-9 continuous-flow liquid helium cryostat (Oxford Instruments). Room temperature EPR spectra were recorded on samples in capillaries. Spin concentrations were measured by double integration of the first-derivative EPR spectra. The resulting areas were compared to the signal from aqueous $Cu(H_2O)_6$ (1mM) recorded with identical instrument settings.[6] EPR simulations were performed with Frank Neese's program, version 1.0 (University of Konstanz, Germany). The framework of the [*g*] and [*A*] tensors were assumed to be collinear.

ENDOR Spectroscopy. ENDOR spectra were recorded on a Bruker ESP3000E spectrometer mounted with a Bruker EN801 X-band cavity and equipped with an ESR-9 continuous-flow liquid helium cryostat (Oxford Instruments). A 500 W ENI amplifier generated the radio frequency.

Mössbauer Spectroscopy. All Mössbauer measurements were performed with a constant acceleration spectrometer calibrated with either hematite or metallic iron, and isomer shifts are reported relative to an Fe metal standard at room temperature. Variable temperature experiments were carried out with the sample placed in the tail section of a variable temperature cryostat. Temperatures of the sample were regulated to within ±0.2 K by a conventional PID (Proportional, Integral, Derivative) system. Using a superconducting magnet, high magnetic fields up to 7.0 T can be applied parallel to the Mössbauer γ-beam. One homemade sample holder able to generate an external magnetic field of 50 mT applied parallel to the γ-rays has been also used.[56] The samples for Mössbauer spectroscopy contained ca. 3.0 mM ^{57}Fe and were sealed in 200 μL nylon cells. The Mössbauer spectra were fitted using the software package WMOSS (WEB Research, Edina, MN).

The analysis was made using the following Hamiltonian **H**:

$$\mathbf{H} = D[\mathbf{S}_z^2 - (^1/_3)S(S+1) + (E/D)(\mathbf{S}_x^2 - \mathbf{S}_y^2)] + \beta_e \mathbf{S}[g]\mathbf{B} + <\mathbf{S}>[A]\mathbf{I} - g_n\beta_n\mathbf{B}\mathbf{I} + \mathbf{H_Q} \quad (4)$$

where D and E are the axial and rhombic zero-field splitting (ZFS) parameters, respectively, β_e is the electronic Bohr magneton, [*g*] is the electronic *g*-tensor, **B** is the magnetic field, <**S**> is the appropriately taken spin expectation value, [*A*] is the magnetic hyperfine tensor, g_n is the nuclear *g*-factor, β_n is the nuclear Bohr magneton, and $\mathbf{H_Q}$ is the quadrupole interaction Hamiltonian. $\mathbf{H_Q}$ is given by

$$\mathbf{H_Q} = (^1/_{12})eQ\mathbf{V}_{\zeta\zeta}[3\mathbf{I}_\xi^2 - {}^{15}/_4 + \eta(\mathbf{I}_\xi^2 - \mathbf{I}_\eta^2)] \quad (5)$$

where the quadrupole interaction is written in the principal axis frame (ξ, η, ζ) of the electric field gradient (EFG) tensor (Q represents the nuclear quadrupole moment, and [V], the EFG tensor). The asymmetry parameter η is defined by the relation:

$$\eta = (V_{\xi\xi} - V_{\eta\eta})/V_{\zeta\zeta} \quad (6)$$

where $|V_{\zeta\zeta}| \geq |V_{\eta\eta}| \geq |V_{\xi\xi}|$ and $0 \leq \eta \leq 1$. The [*A*] and [*g*] tensors are assumed here to be collinear.

Electronic Absorption Spectroscopy. UV−visible spectra were recorded on a Hewlett-Packard 8453 diode array spectrophotometer. The individual spectra of $S_{1/2}$ and S_0 were calculated from the difference of spectra of two samples containing different ($S_{1/2}$:S_0) ratios. According to Mössbauer quantification, the ($S_{1/2}$:S_0) ratios, related to total iron concentration, were (85:15) ± 1% and (51:49) ± 2%. The spectra were normalized to initial iron concentrations ($C_{(85:15)} = 0.25$ mM and $C_{(51:49)} = 0.22$ mM), and the absorbance at any wavelength was expressed as the sum of absorption by $S_{1/2}$ and S_0. The absorption coefficients were determined in the individual spectra of $S_{1/2}$ and S_0: $\epsilon_{410nm\ (S1/2)} = 2600\ M^{-1}\ cm^{-1}$, $\epsilon_{360nm\ (S1/2)} = 1200\ M^{-1}\ cm^{-1}$, $\epsilon_{410nm\ (S0)} = 4000\ M^{-1}\ cm^{-1}$, and $\epsilon_{360nm\ (S0)} = 6400\ M^{-1}\ cm^{-1}$. The details of these calculations can be found in the Supporting Information.

FTIR Spectroscopy. The FTIR spectra were recorded at 4 cm^{-1} resolution, on a Bruker 66 SX spectrometer equipped with a KBr beam splitter and a nitrogen cooled MCT-A (Mercury Cadmium Tellure)

(54) Jansson, M.; Li, Y. C.; Jendeberg, L.; Anderson, S.; Montelione, B. T.; Nilsson, B. *J. Biomol. NMR* **1996**, *7*, 131−141.
(55) Torres, J.; Wilson, M. T. *Methods Enzymol.* **1996**, *269*, 3−11.
(56) Jeandey, C.; Horner, O.; Oddou, J.-L.; Jeandey, C. *Meas. Sci. Technol.* **2003**, *14*, 629−632.

detector. Fur samples in H_2O and in D_2O with ^{14}N and $^{15}N-NO$ were used to record the absorption spectra displayed in Figure 5A and 5B, respectively. The spectra are obtained after subtraction of the infrared absorption of the buffer. The spectra in the 1950 to 1700 cm^{-1} range were obtained with a CaF_2 transmission IR cell of 10 μm path length, defined by a polyethylene spacer. The spectra in the 1800 to 1600 cm^{-1} range were recorded with a 9 reflections ATR system (Attenuated Total Reflection) composed of a diamond crystal and ZnSe optics (DuraSampl*IR* from *SensIR*).

Gel Exclusion Chromatography. The oligomeric states of the apoprotein, FeFur, anf FeFur−NO were determined by analytical gel exclusion chromatography (superdex 75 10/30 Amersham Biosciences) using an FPLC system. The column was equilibrated with 100 mM BTP buffer at pH = 7.5, containing 100 mM KCl and was calibrated using a low molecular weight calibration kit (Amersham Biosciences).

Mass Spectrometry. The NO modified protein was purified using a microspin column (BioRad) in 10 mM ammonium acetate buffer at pH = 7. The mass spectra were recorded on a Micromass Manchester spectrometer equipped with an electrospray ionization source and a TOF-quadrupole detector. The samples were injected by nanospray. Orifice tension was held at 40 V and the interface temperature at 30 °C. The overall charge of the different species was inferred from their respective *m*/*z* value (with z integer) and the mass of Fur as a monomer or a dimer.

Results

EPR Spectroscopy. We reported in a previous paper that the reaction product of NO with FeFur, yielded, in frozen solution, an anisotropic EPR signal $S = {}^1/_2$, associated with an isotropic g value $g_{iso} = 2.03$ and no hyperfine structure.[6] In addition, the EPR spectrum of a sample prepared with ^{15}N enriched NO displayed a narrowing in the low field region, suggesting an interaction of the electronic spin with the NO nitrogen. Nevertheless, no hyperfine structure was resolved. To try to resolve a hyperfine structure, EPR spectra of FeFurNO were recorded at room temperature. In liquid solution, the g strain is generally minimized and the anisotropy of [g] and [A] tensors is averaged, which may help to resolve hyperfine isotropic structure. This procedure has been successfully used with model compounds, to determine weak hyperfine interactions.[57] The spectrum of FeFurNO is only slightly modified when compared to that obtained in frozen solution (Figure 1A). The principal [g] values ($g_1 = 2.042$; $g_2 = 2.032$; $g_3 = 2.017$) are almost unchanged and reveal g anisotropy. The respective line widths (7.0, 5.3, 3.2 G) are smaller than those in frozen solution, but no hyperfine structure is resolved. The spectrum of FeFurNO prepared with ^{57}Fe enriched Fe^{2+} reveals the ^{57}Fe hyperfine structure (Figure 1B). The principal values of the hyperfine tensor, with respect to the [g] framework, [A] (45, 36, 4 MHz), are identical to those obtained in frozen solution.[6]

The absence of the hyperfine structure associated with the $^{14}N(NO)$ probably means that the principal values of the hyperfine tensor are not larger than the corresponding line width. To estimate the maximum values for the $^{14}N(NO)$ hyperfine tensor, the EPR experimental data have been fitted under constraint of one ^{14}N ($I = 1$) hyperfine interaction. A hyperfine contribution from one nitrogen nucleus, in the g_1, g_2 region, cannot exceed 12 MHz, otherwise a hyperfine structure would be detected. In the g_3 region, a hyperfine coupling larger than 6 MHz should be detectable. These results suggest that the maximal principal value of the N(NO) hyperfine tensor must be smaller than 12 MHz in any of the three space directions. Nevertheless, this deduction does not give information about the number of NO's bound to iron. To determine the N(NO) hyperfine tensor, ENDOR spectroscopy was used.

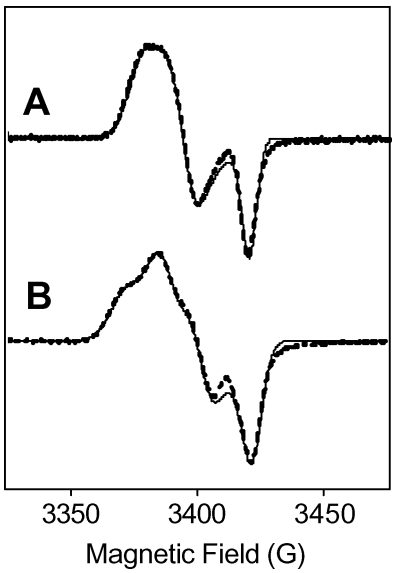

Figure 1. Room temperature X-band EPR spectra of FeFurNO. (A) FeFur protein treated by naturally enriched NO (dashed line). The total protein concentration is 4 mM. The simulation was achieved with the g values (2.042, 2.032, 2.017) using the line widths (7.0, 5.3, 3.2 G) (solid line). (B) FeFur, enriched in ^{57}Fe, and treated by naturally enriched NO (dashed line). The total protein concentration is 3.25 mM. The simulation was achieved with the g values (2.041, 2.032, 2.016), the hfs constants [A] (45, 36, 4 MHz), and the line widths (6.6, 5.5, 4.4 G) (solid line). EPR conditions: microwave frequency, 9.654 GHz; power, 2 mW; amplitude modulation, 1 G; frequency modulation, 100 kHz; room temperature.

ENDOR Spectroscopy. ENDOR spectroscopy is a powerful tool for determination of the hyperfine tensor. This spectroscopic method has already been used in the case of nitrosyl−iron species, such as nitrosyl myoglobin and hemoglobin, to determine the N(NO) hyperfine tensor.[58] The continuous wave X-band ENDOR spectra of FeFurNO were recorded at 50 K in the range of 1 to 50 MHz, for various external "EPR" applied fields within the $g = 2.03$ signal. Two kinds of resonance were observed, corresponding to distinct nuclei. The resonance centered at 14 MHz (not shown) arises from hydrogen nuclei; however the study of this signal is beyond the scope of this paper and will be reported later. The resonances found between 1 and 4 MHz are due to ^{14}N interactions (Figure 2A). The three resonances at 2.4, 3.1, and 3.9 MHz are attributed to nitrogen hyperfine interactions. But, because of the quadrupolar interaction, this pattern of ^{14}N resonances is not amenable to analysis by itself.[59] To identify N(NO) resonances, X-band ENDOR spectra of FeFurNO enriched in $^{15}N(NO)$ were recorded under the same conditions as the unenriched sample (Figure 2B). The spectrum was almost unchanged by the NO enrichment and no new signal was observed and no feature of a ^{15}N hyperfine interaction appeared. The resonances at 3.1 and 3.9 MHz were still present, meaning they are not due to N(NO) hyperfine interaction. The resonance at 2.4 MHz seems to vanish suggesting it was due to $^{14}N(NO)$ nucleus.

(57) Costanzo, S.; Menage, S.; Purrello, R.; Bonomo, R. P.; Fontecave, M. *Inorg. Chim. Acta* **2001**, *318*, 1−7.

(58) Kappl, R.; Hüttermann, J. *Israel J. Chem.* **1989**, *29*, 73−84.
(59) Hoffman, B. M. *Acc. Chem. Res.* **1991**, *24*, 164−170.

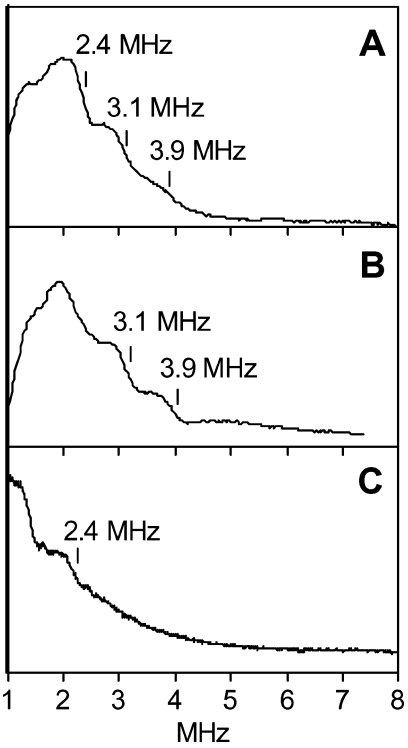

Figure 2. First derivative X-band ENDOR spectra. (A) ENDOR spectrum of FeFur treated by saturated solution of NO gas. The total protein concentration is 5 mM. (B) ENDOR spectrum of FeFur treated by a saturated solution of NO gas enriched in ^{15}N. The total protein concentration is 5 mM. (C) ENDOR spectrum of FeFur enriched in ^{15}N treated by NO from DEANO. The total protein concentration is 4 mM. Conditions: temperature, 50 K; microwave frequency, 9.474 GHz; power, $P = 0.8$ mW; static field, $H = 3318$ G ($g = 2.040$). The spectra that are shown are the first derivatives of absorption spectra as regards to the radio frequency field.

The Fur protein enriched in ^{15}N, reconstituted with Fe^{2+} and treated by NO was studied by ENDOR spectroscopy under the same conditions as the unenriched FeFur (Figure 2C). The spectrum revealed a signal at 1.4 MHz, the Larmor frequency of an ^{15}N nucleus at 340 mT, arising from distant ^{15}N nitrogen nuclei. The signals at 3.1 MHz and at 3.9 MHz had disappeared, which confirmed they arose from the Fur protein. Nevertheless, no signal due to a ^{15}N nucleus is visible, whatever the conditions. The signal at 2.4 MHz was still present, suggesting that it does not derive from a protein atom but instead from the NO nitrogen, as already suggested by the $^{15}N(NO)$ labeling experiments.

Mössbauer Spectroscopy. As reported previously,[18] the zero-field Mössbauer spectrum of ^{57}Fe enriched FeFur solution measured at 4.2 K consists of a quadrupole doublet. The related Mössbauer parameters ($\delta_{/Fe} = 1.19(1)$ mm·s^{-1} and $\Delta E_Q = 3.47(2)$ mm·s^{-1}) are characteristic of a high-spin Fe(II) ion with oxygen and/or nitrogen ligands in an octahedral environment.

Figure 3 (left) shows the Mössbauer spectra of the FeFurNO sample recorded at 77 K in an applied magnetic field of 50 mT (A) and at 4.2 K in an applied magnetic field of 3 T (B) and 7 T (C).

The low-field Mössbauer spectrum (Figure 3A) reveals two distinct components. The first component ((a) in Figure 3A), accounting for 85(1)% of the iron in the sample, exhibits a paramagnetic hyperfine structure. This implies that, at 77 K, the electronic relaxation is slow compared to the Mössbauer time scale. Moreover, the double integration of the $S = {}^1/_2$ EPR signal in the same sample shows that it represents also 85% of total iron in the sample (data not shown).[6] Therefore, we assign the major species to the $S = {}^1/_2$ species detected by EPR spectroscopy which will be referred to as the $S_{1/2}$ species.

The second component, accounting for 15(1)% of the iron in the sample, consists of a sharp quadrupole doublet ((b) in Figure 3A). This species is diamagnetic (see below) and will be referred to as the S_0 species. The related Mössbauer parameters are clearly different from those obtained for the FeFur protein, which suggests that its reaction with NO is complete (Table 3).

The high-field Mössbauer spectra in Figure 3B and 3C have been fitted together within the spin-Hamiltonian formalism in the slow relaxation limit. The solid lines drawn through the spectra in Figure 3 correspond to the best fit obtained with the parameters reported in Table 3. The major species ($S_{1/2}$, solid lines (a) in Figure 3) exhibits the following Mössbauer parameters: $\delta_{/Fe} = 0.20(1)$ mm·s^{-1}, $\Delta E_Q = -0.92(2)$ mm·s^{-1} and $\eta = 0.5(1)$ at 4.2 K. As expected, the principal values of the hyperfine tensor ($A_x = -38$, $A_y = -11$, and $A_z = -50$ MHz) are in agreement with those determined by EPR spectroscopy ($A_1 = 45$, $A_2 = 36$, and $A_3 = 4$ MHz).[6] Indeed, the apparent difference is due to a rotation of the principal axis frames of the $[A]$ and $[g]$ tensors relative to each other.[60] The solid lines (b) are the theoretical curves for the minor species assuming $S = 0$ (see below) and correspond to the following Mössbauer parameters: $\delta_{/Fe} = 0.19(1)$ mm·s^{-1}, $\Delta E_Q = 1.04(2)$ mm·s^{-1} and $\eta = 0.9(1)$ at 4.2 K, assuming $S = 0$.

The proportion of S_0 increases when equilibration of the starting apo-protein in the anaerobic atmosphere is reduced from one night to a few hours (see Experimental Section). To further characterize S_0, a new sample with an increased percentage of S_0 was prepared. This sample has been studied by Mössbauer spectroscopy at 4.2 K under an applied magnetic field of 50 mT and 7.0 T, as shown in Figure 3 (right). The Mössbauer spectra (Figure 3D and 3E) were fitted within the spin-Hamiltonian formalism in the slow relaxation limit, and the solid lines drawn through the experimental spectra correspond to the best fit obtained with the parameters reported in Table 3. A satisfactory fit was obtained when assuming $S = 0$ for simulating the contribution of S_0 (49(2) % of the iron in the sample, solid lines (b) in Figure 3 (right)). The pattern of spectrum b in Figure 3E indicates a value of the asymmetry parameter close to 1. $S_{1/2}$ contributes here to 51(2)% of the total spectra (solid lines (a) in Figure 3 (right)).

Electronic Absorption Spectroscopy. The electronic absorption spectrum of FeFurNO exhibited intense bands in the UV region and weaker bands in the visible region (not shown). Analyses of various samples containing different ratios of $S_{1/2}$ and S_0 revealed specific features of the two species. In particular, the increase of the S_0 concentration is concomitant with an increase of the absorption at 360 nm. The determination of their relative proportion from Mössbauer experiments allowed us to deconvolute the individual spectra of $S_{1/2}$ and S_0 (Figure 4). The spectrum of $S_{1/2}$ is characterized by a band at $\lambda_{max} = 410$ nm ($\epsilon = 2.5(1) \times 10^3$ M^{-1} cm^{-1}), with a shoulder at $\lambda_{max} = 540$ nm, and two bands at 650 nm ($\epsilon = 310$ M^{-1} cm^{-1}) and 830 nm ($\epsilon = 270$ M^{-1} cm^{-1}). The spectrum of S_0 is composed

(60) Popescu, V. C.; Münck, E.; Fox, B. G.; Sanakis, Y.; Cummings, J. G.; Turner, I. M., Jr.; Nelson, M. J. *Biochemistry* **2001**, *40*, 7984−7991.

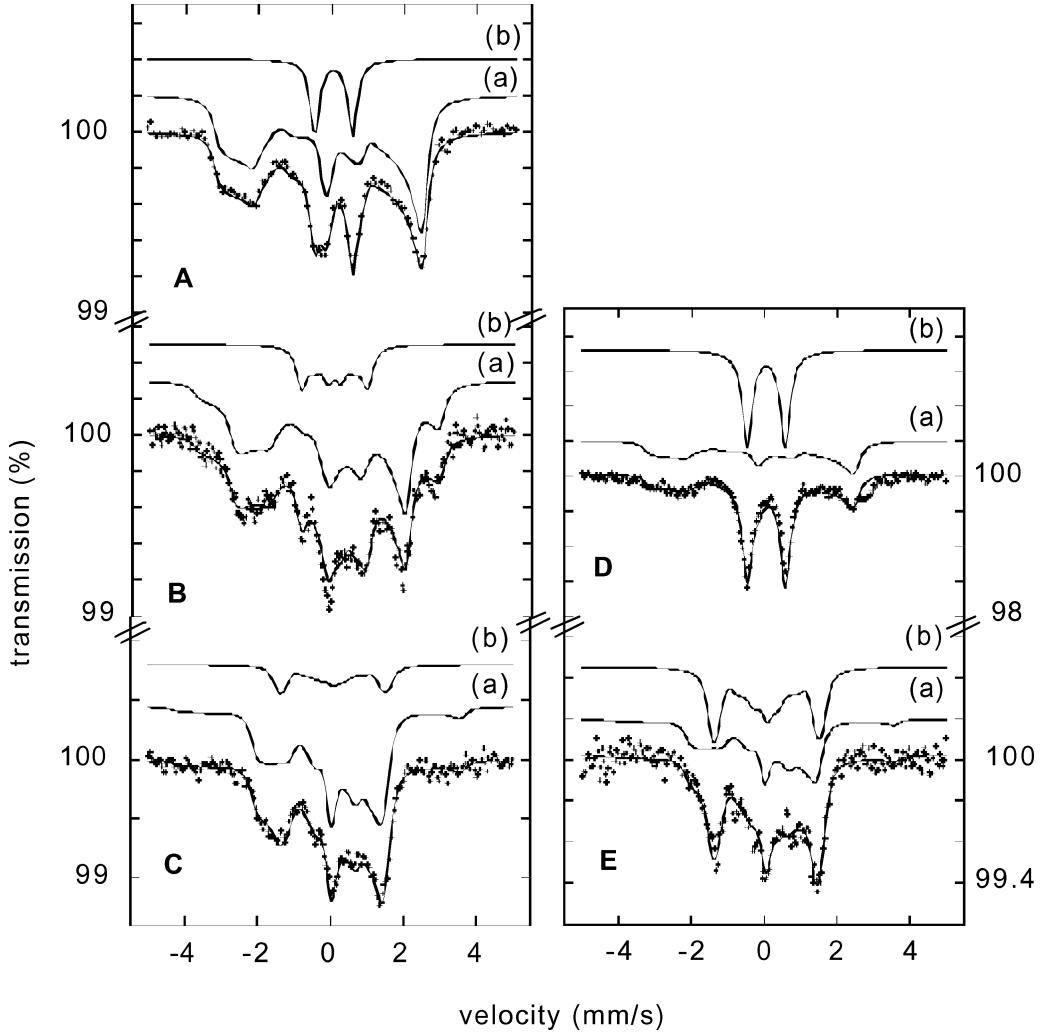

Figure 3. Applied-field Mössbauer spectra of ^{57}FeFurNO Mössbauer spectra of ^{57}FeFurNO (from a solution of 3.25 mM ^{57}FeFur in 100 mM BisTris propane buffer at pH = 7.5 containing 100 mM KCl) in various magnetic fields applied parallel to the γ-rays. Left panel (sample containing 85(1)% of $S_{1/2}$ and 15(1)% of S_0): (A) $T = 77$ K, $H = 50$ mT, (B) $T = 4.2$ K, $H = 3.0$ T, (C) $T = 4.2$ K, $H = 7.0$ T. Right panel (sample containing 51(2)% of $S_{1/2}$ and 49(2)% of S_0): (D) $T = 4.2$ K, $H = 50$ mT, (E) $T = 4.2$ K, $H = 7.0$ T. The experimental spectra were fitted (solid curves drawn through the data) with the parameter set of Table 3. The solid curves above the experimental spectra show the contribution of each iron species ((a) $S_{1/2}$, (b) S_0).

Table 3. Mössbauer Parameters for S_0 and $S_{1/2}$ Species at 4.2 K

	$S_{1/2}$	S_0
S	$^1/_2$	0
g_1	2.015[a]	2.0
g_2	2.032[a]	2.0
g_3	2.042[a]	2.0
A_x (MHz)	−38(1)	
A_y (MHz)	−11(1)	
A_z (MHz)	−50(1)	
A_{iso} (MHz)	−33(1)	
$\delta_{/Fe}$ (mm·s^{-1})		
4.2 K	+0.20(1)	+0.19(1)
77 K	+0.16(1)	+0.14(1)
ΔE_Q (mm·s^{-1})		
4.2 K	−0.92(2)	1.04(2)
77 K	−0.82(2)	1.04(2)
η	0.5(1)	0.9(1)

[a] From EPR spectroscopy.

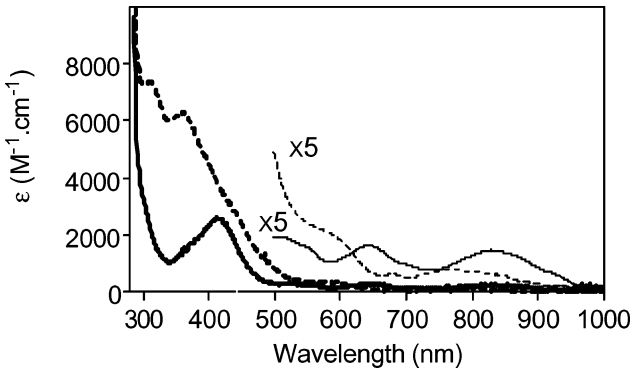

Figure 4. UV−visible spectra of $S_{1/2}$ and S_0. The individual spectra of $S_{1/2}$ (solid line) and S_0 (dashed line) were calculated, as described in the Experimental Section. The upper curves have been multiplied 5-fold in the range 500 to 1000 nm.

of two bands in the UV region at $\lambda_{max} = 310$ nm ($\epsilon = 7.3(2) \times 10^3$ M^{-1} cm^{-1}) and $\lambda_{max} = 360$ nm ($\epsilon = 6.2(2) \times 10^3$ M^{-1} cm^{-1}), with a shoulder at $\lambda_{max} = 590$ nm, and a band at $\lambda_{max} = 790$ nm ($\epsilon = 130$ M^{-1} cm^{-1}). In the following experiments, the measurements of the absorbance at 410 and 360 nm were used to determine the concentrations of $S_{1/2}$ and S_0 in our samples (see Experimental Section).

Fourier Transform Infrared Spectroscopy (FTIR). The infrared absorption spectrum of FeFurNO was recorded between 1950 and 1700 cm^{-1} for the sample in H_2O (Figure 5A), 1800 and 1650 cm^{-1} for the sample in D_2O (Figure 5B and 5C). This

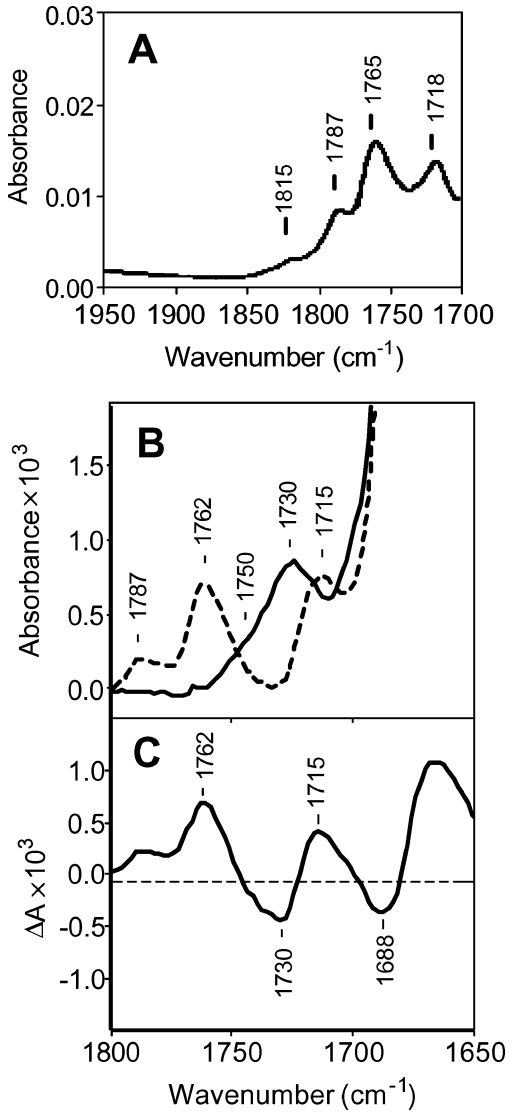

Figure 5. FTIR spectra of the FeFurNO. (A) Difference spectrum of FeFur protein at 2 mM in H_2O, treated minus untreated by NO. The sample contained 85% $S_{1/2}$, according to UV−visible spectroscopy. (B) Spectra of FeFur protein in D_2O, at a final concentration of 6 mM, modified by natural (dashed line) and ^{15}N enriched (solid line) NO gas. The samples contained 80% $S_{1/2}$, according to UV−visible spectroscopy. (C) Difference spectrum of the FeFur protein modified by natural NO minus ^{15}N enriched NO.

spectrum revealed two main bands at 1765 and 1718 cm^{-1} and two weaker ones at 1815 and 1787 cm^{-1}. In this region, except from IR modes of protonated Asp and Glu carboxylic side chains, usually contributing in the 1740−1700 cm^{-1} range,[61,62] only the IR stretching mode from NO is expected to contribute. In a parallel experiment using the FTIR-ATR system, DEANO was added directly to the cell containing an FeFur sample and the FTIR spectra recorded as a function of time, which revealed that the *in situ* reaction of Fur with NO led to the appearance of the bands at 1787, 1765, and 1718 cm^{-1} (not shown). This ATR system does not allow the analysis above 1800 cm^{-1} due to the infrared absorption of diamond. The FTIR absorption spectrum of FeFur in D_2O treated by NO gas also shows the three bands at almost the same frequencies (Figure 5B). More precisely, the two modes at 1765 and 1718 cm^{-1} are slightly downshifted by 3 cm^{-1} to 1762 and 1715 cm^{-1}. It is not possible however to deduce that it is a direct effect of the H_2O/ D_2O exchange on the mode itself or a downshift induced by slight changes in background absorption of the sample. The FTIR spectrum of FeFur in D_2O treated by ^{15}N enriched NO gas exhibits one main band at 1730 cm^{-1} with a shoulder at ∼1750 cm^{-1} (Figure 5B). The difference spectrum calculated from the absorption spectra of samples prepared with natural abundance NO and ^{15}N enriched NO suggested the presence of another band in the ^{15}NO spectrum, at 1688 cm^{-1} (Figure 5C). In the absorption spectrum of Figure 5B solid line, this band is hidden below the dominating peptide absorption bands. The disappearance of the bands at 1787 and 1762 cm^{-1} upon ^{15}N—NO labeling confirm their assignment to the ν(N═O) IR mode. The band at 1715 cm^{-1} is also at least partly suppressed upon ^{15}NO labeling. The theoretical stretching frequencies ratios of the ^{15}N labeled NO group, as regard to ^{14}NO, were determined using the approximation of a diatomic harmonic oscillator. The downshift expected for the ν(NO) IR mode upon ^{15}NO labeling is then estimated at 30−35 cm^{-1}. The bands at 1787 cm^{-1} (weak), 1762 cm^{-1}, and 1715 cm^{-1} were thus expected to shift to ∼1755 cm^{-1}, ∼1730 cm^{-1}, and ∼1685 cm^{-1} upon ^{15}N labeling. These values are very close to those observed: 1750 cm^{-1} (sh), 1730 cm^{-1}, and 1688 cm^{-1}. The effect of ^{15}NO labeling on the bands observed in the 1800−1700 cm^{-1} region is best interpreted as a downshift by ∼32 cm^{-1} of the two main bands at 1762 cm^{-1} and 1715 cm^{-1} to 1730 cm^{-1} and possibly to 1688 cm^{-1}.

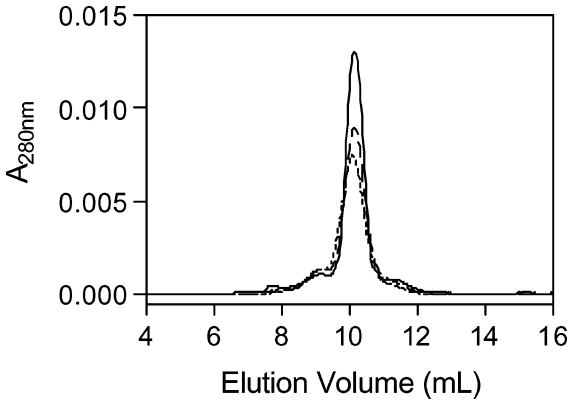

Figure 6. Gel exclusion chromatography. Gel exclusion chromatograms of apo-Fur protein at 1 mM (dotted line), FeFur protein at 1 mM (dashed line), and FeFurNO at 1 mM (bold line). A volume of 200 μL of protein solution was loaded on the Superdex 75 at a flow rate of 1 mL/ min, at 4 °C, and the elution of the proteins was monitored at 280 nm.

Gel Exclusion Chromatography. The effect of NO treatment on the oligomeric state of FeFur was assessed by gel exclusion chromatography (Figure 6). The chromatograms of the apoprotein and FeFur solutions exhibit one main peak at an elution volume, V_e = 10.2 mL, corresponding to an apparent molecular weight of 36 kDa. Likewise, the chromatogram of the FeFur−NO solution is composed of one main peak characterized by an elution volume, V_e = 10.2 mL, only compatible with a dimer.

Mass Spectrometry. Under nondenaturating conditions, the mass spectrum of FeFurNO is composed of distinct peak groups, corresponding to different positively charged species (Figure 7A). Two different oligomeric states can be distinguished. The group of peaks centered at an *m*/*z* around 3060 can only arise from a +11 charged dimer. The assignment as a monomer was

(61) Venyaminov, S.; Kalnin, N. N. *Biopolymers* **1990**, *30*, 1243−1257.
(62) Barth, A. *Prog. Biophys. Mol. Biol.* **2000**, *74*, 141−173.

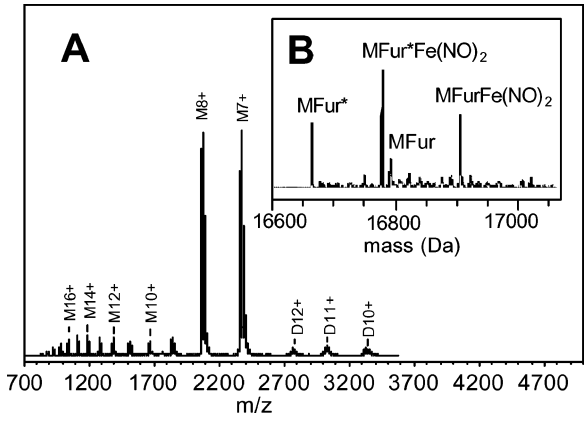

Figure 7. Mass spectra of nondenaturated FeFurNO. (A) FeFur protein modified by NO at 3.5 mM, containing 85% of $S_{1/2}$. The sample was injected at a concentration of 10 μM using a nanospray ionization source; the orifice tension was 40 V, and the interface temperature, 30 °C. The dimeric and monomeric forms and their related charge are noted Dz+ and Mz+, respectively. (B) Reconstituted spectrum using the peaks of the monomer. M and M* represent the monomeric Fur protein (without zinc ion) with and without N-terminal methionine, respectively. $Fe(NO)_2$ represents a mass increase of +116(2) Da.

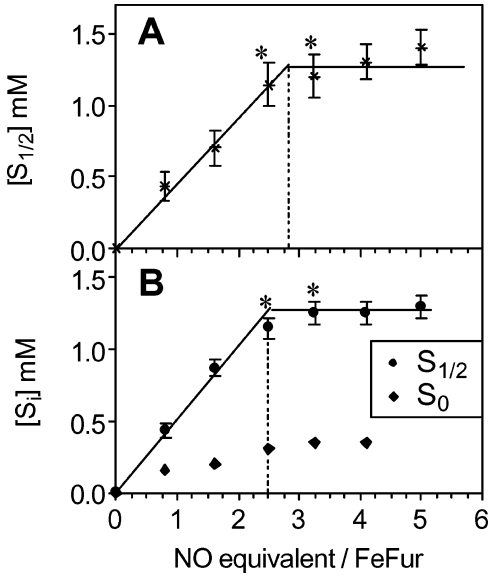

Figure 8. Stoichiometry of the reaction between NO and FeFur. The FeFur protein was exposed to DEANO by six successive additions. The concentrations of $S_{1/2}$ and S_0 were plotted versus the sum of NO equivalent as regards to initial FeFur concentration. (A) EPR quantification of the $g = 2.03$ signal. EPR conditions: microwave frequency, 9.654 GHz; power, 5 μW; amplitude modulation, 4 G; frequency modulation, 100 kHz; temperature, 30 K. (B) UV−visible quantification of $S_{1/2}$ and S_0 concentrations. The concentration of free NO in the reaction mixture was measured at two steps of the reaction, as noted by an asterisk. Before the breakpoint [NO] = 0.1 mM and after the breakpoint [NO] = 1.5 mM.

ruled out because it leads to a non integer value of +5.5 for the charge. The dimer is also visible in the groups of peaks at an *m*/*z* around 2800 and 3400, but the latter are superimposed with peaks of a monomer species. All groups of peaks at an *m*/*z* between 800 and 2400 are almost exclusively monomer species. Under the conditions of the experiment, it is difficult to maintain the dimeric form of the protein. The mass spectrum was reconstituted from the peaks of the monomer (Figure 7B). This reconstituted spectrum showed two couples of masses (16 660, 16 790 Da) and (16 776, 16 907 Da), each containing two forms of the protein: with and without N-terminal methionine (noted by an asterisk).[63] The first couple of masses (16 660, 16 790 Da) corresponds to a monomer which does not contain the structural zinc. The second couple (16 776, 16 907 Da) is characterized by a mass increase of $\Delta m = +116(2)$ Da, which is only compatible with one Fe and two NO's (denoted $Fe(NO)_2$).

Fe/NO Stoichiometry. To obtain information about the nature of $S_{1/2}$ and S_0, the reaction of FeFur with NO was followed by EPR and UV−visible spectroscopies. First, the concentration of NO following the decomposition of DEANO was determined, with 5% accuracy, using horse heart myoglobin. Next, the reaction of NO with FeFur, after successive additions of known DEANO amounts, was followed by EPR (Figure 8A) and UV−visible (Figure 8B) spectroscopies. The concentrations of $S_{1/2}$ and S_0 were plotted versus the concentration ratio $[NO]/[Fe^{2+}]_{initial}$. The $S_{1/2}$ concentration increased linearly with the amount of DEANO added, until all the starting FeFur protein had reacted. The proportion of $S_{1/2}$ was then 80% of the initial iron concentration, and an excess of NO did not modify the ($S_{1/2}$:S_0) ratio. The breakpoint gave us a stoichiometry of 2.5−2.7 NO/Fe, for the mixture of $S_{1/2}$ and S_0 species.

In addition, the concentration of free NO in the reaction mixture was assessed, using the myoglobin assay, before and after the breakpoint (as noted by asterisks). The free NO concentration in the reaction mixture, after three successive additions of 1.7 mM of NO (2.5 equiv of NO/Fe), was 0.1 mM. In contrast, the concentration of free NO measured just after the breakpoint was 1.5 mM.

EPR Studies of the C132G and C132G, C137G Variants. The EPR and UV−visible features of $S_{1/2}$ are remarkably similar to those of bis-thiolato dinitrosyl−iron complexes,[57,64] raising the possibility that NO releases the iron from the regulatory site and forms a dinitrosyl−iron complex with two cysteines of Fur. *Escherichia coli* Fur contains four cysteines (C92, C95, C132, and C137); two of them, C92 and C95, are known to be bound to the structural zinc site in the dimer,[51,52] and the two others, C132 and C137, are reduced and easily accessible to alkylating agents.[52] Two variants of the Fur protein were constructed by site directed mutagenesis, the single mutant C132G and the double mutant C132G, C137G. Both variants were reconstituted with ^{57}Fe enriched Fe^{2+}. The DNA protection assay[6] revealed that they bind DNA similarly to the wild-type Fur (not shown).

The EPR spectra of the FeFurNO variants were recorded at 30 K. Both spectra show only a signal in the $g = 2$ region. The principal [*g*] values of the NO modified C132G mutant (2.042, 2.033, 2.015) and of the NO modified C132G, C137G mutant (2.042, 2.035, 2.015) are almost identical to those of the wild type. The ^{57}Fe hyperfine tensors of both variants, [*A*] = (50, 39, 10 MHz) and [*A*] = (48, 38, 11 MHz), respectively, are very close to that of the wild-type protein. The principal values of the ^{57}Fe hyperfine tensors and the respective line widths, 9.2, 7.6, 5 G and 8.5, 8.5, 5 G, are somewhat larger, but they are still very close to the values determined for the wild type.

(63) Michaud-Soret, I.; Adrait, A.; Jaquinod, M.; Forest, E.; Touati, D.; Latour, J. M. *FEBS Lett.* **1997**, *413*, 473−476.

(64) Boëse, M.; Mordvintcev, P. I.; Vanin, A. F.; Busse, R.; Mulsch, A. *J. Biol. Chem.* **1995**, 270, 29244−29249.

This suggests that the cysteines 132 and 137 are not ligands of the iron in the dinitrosyl−iron $S_{1/2}$ species.

Discussion

We showed through in vitro and in vivo experiments that NO inhibition of Fur involves its binding to the iron center of FeFur and results in a spin $S = {}^1/_2$ species which represents 85% of the total iron and gives an EPR signal at $g = 2.03$. In addition, we showed that this EPR signal is still present in the protein fraction after gel exclusion chromatography, which indicates that the nitrosyl−iron unit is coordinated to the Fur protein. NO binding to the iron center was proposed to induce a conformational change responsible for the protein inhibition.[6] To obtain a deeper understanding of the inhibition mechanism, it was necessary to determine the nature and the electronic structure of the Fur-bound nitrosyl−iron species. As illustrated in the recent chemical literature, assessing the electronic structure of nitrosyl−iron species is quite a challenging task. Two kinds of nitrosyl−iron species have been reported to possess a spin $S = {}^1/_2$ ground state: the mononitrosyl $\{Fe(NO)\}^7$ and the dinitrosyl $\{Fe(NO)_2\}^9$ units. As detailed in Tables 1 and 2, they possess different spectroscopic properties which are akin to their respective Fe−NO bonding mode and spin distribution. The $\{Fe(NO)\}^7$ species are characterized by a single nitrosyl stretching vibration ν_{NO} in the range 1620−1730 cm^{-1}. In addition, they exhibit a small ^{57}Fe hyperfine coupling ($A_{iso}(^{57}Fe) < 15$ MHz) and a large $^{14}N_{(NO)}$ hyperfine coupling ($A_{iso}(^{14}N_{(NO)}) > 30$ MHz), in agreement with the major spin density residing on the nitrosyl ligand. By contrast, the $\{Fe(NO)_2\}^9$ species possess two nitrosyl vibrations ν_{NO} in the range 1680−1810 cm^{-1}, a large ^{57}Fe hyperfine coupling ($A_{iso}(^{57}Fe) > 30$ MHz) and a small $^{14}N_{(NO)}$ hyperfine coupling ($A_{iso}(^{14}N_{(NO)}) < 15$ MHz). To assign one of the two forms to the FeFur nitrosyl adduct, we investigated its spectroscopic properties using a combination of magnetic (EPR, ENDOR, Mössbauer) and optical (UV−visible, FTIR) techniques, gel exclusion chromatography, mass spectrometry, and NO binding titration. The first result that emerged from these studies was the finding through Mössbauer spectroscopy that NO reaction with FeFur produces a second and minor (15%) species which is assigned an $S = 0$ ground spin state, in agreement with the fact that it is not detected by EPR. Therefore, combined spectroscopic studies now allow the whole FeFur iron interacting with NO to be accounted for. FTIR supports that this minor species is probably also a nitrosyl−iron species, and its spectroscopic properties will be discussed in order to fully understand the interaction of FeFur with NO.

Electronic Structure of FurFeNO Species. A. EPR, ENDOR, and Mössbauer Spectroscopies of the $S_{1/2}$ Species. EPR spectra of the NO modified FeFur protein were recorded at room temperature to resolve a nitrogen hyperfine structure. Nevertheless, the EPR spectra still exhibit g anisotropy, and g strain is not decreased enough to allow for the resolution of any hyperfine structure. In liquid media, this remaining anisotropy is commonly observed with large molecules such as proteins which reduce free tumbling. Therefore, the principal values of the N(NO) hyperfine tensor are probably less than 12 MHz; otherwise a hyperfine structure should be apparent in the EPR spectra. The ^{15}N labeling experiments suggest that the ENDOR resonance at 2.4 MHz may arise from coupling to nitrosyl N(NO). Although the hyperfine structure cannot be resolved, the absence of N(NO) resonance at frequencies higher than 2.4 MHz is consistent with the hypothesis of principal values of the hyperfine tensor ($A(^{14}N_{(NO)})$ smaller than 12 MHz.

The EPR spectrum of the NO modified FeFur protein prepared with Fe^{2+} enriched in ^{57}Fe shows the ^{57}Fe hyperfine interaction. The principal values of the hyperfine tensor, $[A] =$ (45, 36, 4 MHz), are identical to those found in frozen solution.[6] The value of 45 MHz is larger than any of the principal values reported for ^{57}Fe hyperfine tensors of $\{Fe(NO)\}^7$ ($S = {}^1/_2$) complexes. Consistently, Mössbauer spectroscopy allowed us to estimate $|A_{iso}(^{57}Fe)| = 33(1)$ MHz for $S_{1/2}$. It appears then that $S_{1/2}$ possesses a large $A_{iso}(^{57}Fe)$ and a small $A(^{14}N_{(NO)})$, two features characteristic of the $\{Fe(NO)_2\}^9$ electronic structure.

B. Fourier Transform Infrared Spectroscopy (FTIR). The FTIR signal is composed of two main bands at $\nu = 1762$ cm^{-1}, $\nu = 1715$ cm^{-1} and two weaker bands at $\nu = 1787$ cm^{-1}, $\nu =$ 1815 cm^{-1}. In the FTIR spectrum of ^{15}N enriched FurFeNO, the three bands vanish and are replaced by one band at $\nu =$ 1730 cm^{-1} with a shoulder at around 1750 cm^{-1}. Another band at $\nu = 1688$ cm^{-1} can be detected only in the $^{14}N-^{15}N$ difference spectrum. Literature data show that NO stretching frequencies are downshifted by ca. 32 upon ^{15}N NO labeling. This supports the assignment of the three bands at 1715, 1762, 1787 cm^{-1} to NO stretching vibrations. No counterpart of the higher energy band at 1815 cm^{-1} could be detected at ca. 1782 cm^{-1} even in the $^{14}N-^{15}N$ difference spectrum. This may be due to the low intensity of this band and the presence of the strong 1787 cm^{-1} band in the ^{14}NO spectrum. It is therefore likely that all these bands correspond to stretching vibrations of NO groups. Nevertheless, the heterogeneity of the sample does not allow an immediate unambiguous assignment of the NO stretching frequencies to either $S_{1/2}$ or S_0. These bands were tentatively assigned to the $S_{1/2}$ and S_0 species from the correlation of their relative intensities with the concentration of $S_{1/2}$ and S_0. According to UV−visible quantification, the ^{15}N and ^{14}N NO treated FeFur samples used for FTIR contained 80 to 85% of $S_{1/2}$. We thus tentatively assigned the two main bands sensitive to ^{15}NO labeling, at 1762 and 1715 cm^{-1}, to the ν-(NO) IR modes of two NO molecules in the $S_{1/2}$ species. It is possible that the small band at 1787 cm^{-1} which shifts to 1750 cm^{-1} came from an Fe-bound NO from the S_0 species. The identification of two distinct NO stretching frequencies for $S_{1/2}$ is again in favor of a dinitrosyl−iron structure. Moreover, a stretching frequency of 1762 cm^{-1} is out of the range observed for $\{Fe(NO)\}^7$ complexes (Table 1) while it fits very well the frequency range determined for $\{Fe(NO)_2\}^9$ complexes (Table 2).

Electronic Structure of the S_0 Species. While the $S_{1/2}$ species can be safely assigned an $\{Fe(NO)_2\}^9$ electronic structure, the situation is less clear for the S_0 species. Indeed, its diamagnetic nature and its low content in the FeFur nitrosyl species complicate the spectroscopic analysis. Moreover, five kinds of nitrosyl−iron complexes have been shown to possess a diamagnetic ground state. These are three mononitrosyl and two dinitrosyl species with $\{Fe(NO)\}^6$, $\{Fe(NO)\}^8$, $\{Fe(NO)\}^{10}$, $\{Fe(NO)_2\}^8$, and $\{Fe(NO)_2\}^{10}$ electronic structures. Only the former two have been characterized in depth through many examples. The $\{Fe(NO)\}^6$ species possess a small isomer shift $\delta \approx 0$ $mm \cdot s^{-1}$ and values of the NO stretching frequency

spanning a wide range around $\nu_{NO} \approx 1850$ cm^{-1}.[33,34,65,66] Two kinds of {Fe(NO)}^{8} species have been reported. One associating Π-acceptor ligands have small values of the isomer shift ($\delta \sim 0$ mm·s^{-1}) and NO stretching frequencies in a narrow range at 1700−1770 cm^{-1}.[33,67−69] Another complex with a nitrogen ligand exhibits an isomer shift of 0.27 mm·s^{-1}, but its NO stretching frequency is supposed to be very low ($\nu_{NO} < 1500$ cm^{-1}).[33] Some {Fe(NO)$_2$}^{10} species have been reported.[43,44,70] The isomer shifts range from $\delta = 0.2$ to 0.3 mm·s^{-1}, but the NO stretching frequencies are below 1760 cm^{-1}. The NO stretching frequencies potentially associated to S_0 ($\nu_{NO} = 1787$ and 1815 cm^{-1}) are below those observed for {Fe(NO)}^{6} complexes and above those of {Fe(NO)}^{8} and {Fe(NO)$_2$}^{10} complexes, but they belong to the range observed for several diamagnetic dinitrosyl {Fe(NO)$_2$}^{8} complexes,[27,34] suggesting that S_0 may possess an {Fe(NO)$_2$}^{8} electronic structure. Unfortunately, to the best of our knowledge, no Mössbauer parameters of {Fe(NO)$_2$}^{8} complexes are yet available for comparison. The isomer shift value of S_0 ($\delta_{/Fe} = 0.19(1)$ mm·s^{-1}) is close to the value determined for $S_{1/2}$ ($\delta_{/Fe} = 0.20(1)$ mm·s^{-1}). This indicates that the electronic density at the iron nucleus is similar for the two species and that they differ only by the nature of the nitrosyl ligands as inferred from FTIR data.

Gel Exclusion Chromatography and Mass Spectrometry. Gel exclusion chromatography reveals that the reaction with NO does not break the dimeric structure of FeFur, and it is known that the dimeric form contains the structural zinc ion[51,52]. The mass spectrum of FeFurNO reveals the presence of dimeric forms and also monomeric forms that do not contain the structural zinc ion. As the protein is in the dimeric form before injection, the dissociation of the dimer and the loss of the zinc ion are due to the conditions used in mass spectrometry experiments, as assessed by gel exclusion chromatography. The analysis of the monomer peaks allowed us to characterize the modifications caused by NO. The mass increase of 116 Da readily accounts for the presence of one Fe and two NO, which is best explained by the coordination of an Fe(NO)$_2$ unit to the Fur protein. Thus, in combination with FTIR, mass spectrometry shows that two NO are coordinated to the iron.

These spectroscopic and spectrometric studies are informative on the structure of $S_{1/2}$ in comparison with model compounds.

Fe/NO Stoichiometry. The reaction of NO with FeFur was monitored by EPR and UV−visible spectroscopies. Quantification of the $S_{1/2}$ and S_0 concentrations shows that the reaction is complete with 2.5−2.7 equiv of NO per iron ion. The average value is closer to 3 equiv of NO rather than 2 equiv. Moreover, the myoglobin assay reveals that there is essentially no free NO until 2.6(1) equiv per iron have been added. Assuming that two NO's ($S = {}^1/_2$) bind to one Fe(II) ($S = 2$) would lead to an integer spin species. To take into account the paramagnetic nature of $S_{1/2}$, the reaction would consume an additional electron. It has previously been reported that NO may behave as a reductant.[71,72] Therefore, using two NO molecules as iron ligands and a third one as an electron donor may explain the observed stoichiometry approaching three NO molecules per iron ion. Furthermore, the addition of an excess of NO does not convert S_0 to $S_{1/2}$, suggesting that the formation of $S_{1/2}$ is not a direct reduction of S_0 by NO. Nevertheless, the spectroscopic studies suggest that S_0 may be a dinitrosyl {Fe(NO)$_2$}^{8} species which is a potential intermediate in the formation of $S_{1/2}$. It is thus possible that the ligand frameworks of $S_{1/2}$ and S_0 are different and that the reduction by NO is allowed only with the ligand set of $S_{1/2}$. Alternatively, the two species may possess the same ligand framework, but the reduction step by NO would involve an early intermediate, as for example a mononitrosyl species and not the dinitrosyl {Fe(NO)$_2$}^{8} species, S_0.

Summary and Biological Implications

The present results show that the interaction of NO with Fe−Fur produces two nitrosyl−iron species: a major one with an {Fe(NO)$_2$}^{9} ($S = {}^1/_2$) electronic structure and a minor one with an $S = 0$ ground state for which an {Fe(NO)$_2$}^{8} electronic structure is preferred, although an alternate {Fe(NO)}^{6} structure cannot be totally excluded.

In addition, titration of free NO in the reaction mixture suggested that deoxyMb is not able to displace NO from the FeFurNO. The affinity of NO for myoglobin is probably smaller than that for FeFur, since myoglobin is able to quantify the free NO but not to displace the nitrosyl ligand FurFeNO. This stability is further shown by the mass spectrometry experiments which reveal that the nitrosyl iron unit is retained.

The dinitrosyl structure of $S_{1/2}$ involves that at least two Fur−Fe(II) bonds have been broken, leading to a six-coordinated dinitrosyl−iron complex. The structures of the {Fe(NO)$_2$}^{9} complexes reported in the literature are mainly four-coordinated, and a few examples of five-coordinated complexes have been reported. Therefore, it is possible that the binding of NO induces a significant reorganization of the iron site, leading to a four- or five-coordinated iron species, with two NO ligands. In this scheme, the reaction with NO would break three or four Fur−Fe(II) bonds. The knowledge of the remaining ligands is crucial to understanding the basis of the conformational change. ENDOR spectroscopy reveals the presence of nitrogens, but we cannot infer whether they are actual donor atoms to the iron. A major reorganization of the iron site could lead to the release of the stable Fe(NO)$_2$ from the regulatory site and its binding to cysteinate residues of the protein. Indeed, the EPR features of $S_{1/2}$ have been repeatedly associated to the presence of thiolate sulfur in the coordination sphere of dinitrosyl−iron complexes. The similarity of the electronic absorption spectra of the nitrosylated Fur with those of thiolato iron compounds made such an hypothesis attractive. The studies of the C132G mutant and the C132G, C137G double mutant demonstrate that thiolate groups of these cysteines are not ligands of the dinitrosyl−iron complex. The retention of the dimer structure of Fur in the nitrosyl adduct warrants that the two other Fur cysteines, C92 and C95, are not involved in iron coordination, as they are already ligands of the zinc ion in the structural zinc site. Therefore, sulfur can be excluded as a donor atom of iron of

(65) Schünemann, V.; Benda, R.; Trautwein, A. X.; Walker, F. A. *Israel J. Chem.* **2000**, *40*, 9−14.
(66) Gerbeleu, N. V.; Arion, V. B.; Simonov, Y. A.; Zavodnik, V. E.; Stavrov, S. S.; Turta, K. I.; Gradinaru, D. I.; Birca, M. S. *Inorg. Chim. Acta* **1992**, *202*, 173−181.
(67) Albertin, G.; Bordignon, E. *Inorg. Chem.* **1984**, *23*, 3822−3825.
(68) Di Vaira, M.; Ghilardi, C. A.; Sacconi, L. *Inorg. Chem.* **1976**, *15*, 1555−1561.
(69) Hoffman, P. R.; Miller, J. S.; Ungermann, C. B.; Caulton, K. G. *J. Am. Chem. Soc.* **1973**, *95*, 7902−7904.
(70) Albano, V. G.; Araneo, A.; Bellon, P. L.; Ciani, G.; Manassero, M. *J. Organomet. Chem.* **1974**, *67*, 413−422.
(71) Vanin, A. F.; Liu, X.; Samouilov, A.; Stukan, R. A.; Zweier, J. L. *Biochim. Biophys. Acta* **2000**, *1474*, 365−377.
(72) Wang, Y.; Averill, B. A. *J. Am. Chem. Soc.* **1996**, *118*, 3972−3973.
(73) Herold, S.; Exner, M.; Nauser, T. *Biochemistry* **2001**, *40*, 3385−3395.

$S_{1/2}$, which shows that these EPR-based conclusions do not apply to all protein-bound dinitrosyl−iron complexes.

Although at the moment spectroscopic studies have not positively identified the iron ligands of the dinitrosyl−iron center, structural hypotheses can be proposed from the X-ray structure of Fur. A reasonable assumption is that the water molecule bound to the iron in FeFur should be the easiest ligand to be displaced by NO. Although the water molecule is more strongly bound than the second oxygen of the bidentate carboxylate Asp-88, its replacement by an incoming ligand is not hindered by any protein structural change. It is likely then that the formation of a mononitrosyl−iron center, by exchange of the water molecule with NO, would not trigger a conformational motion. On the other hand, the formation of the dinitrosyl−iron unit may involve, at the very least, a carboxylate shift of Asp-88 and possibly the release of one or more protein ligands. Such a reorganization should be sufficient to induce a conformational change of the protein. Thus, the formation of the dinitrosyl−iron center is probably required to trigger the conformational change responsible for NO inhibition of Fur−Fe.

Our in vivo and in vitro experiments have clearly linked the inactivation of FeFur to the formation of $S_{1/2}$. The present finding of S_0 raises the question: is S_0 an inhibited form of the protein? The results of the Fur binding activity assay have shown that NO is able to dissociate the FurFe/DNA complex formed from 20 μM FeFur and 50 nM DNA. It is likely that, under these conditions, S_0 would also be generated. Assuming a minimum quantity of 15% of S_0 would lead to 3 μM of Fur protein in S_0 form. If S_0 was active, this residual activity should be detected, as DNA binding activity is already observed with 2 μM of FeFur in the presence of 50 nM DNA. Thus both species, $S_{1/2}$ and S_0, are probably inactive forms of the protein. For a more complete understanding, the question of a possible specific derepression of genes by one or the other form, S_0 and $S_{1/2}$, should be considered.

Acknowledgment. We thank Victor Duarte and Nadia Abed for help in the preparation of the Fur mutants, Anne Gonzalez de Peredo for the mass spectrometry analysis, and Pierre Bonville and Nadine Genand-Riondet (CEA/Saclay) are gratefully acknowledged for the in-field Mössbauer experiments. This work was supported by Grant 0202069401 from the Région Rhône-Alpes.

Supporting Information Available: Description of the method for MbNO concentration determination and detail of the calculations used in the electronic absorption spectroscopy analysis. This material is available free of charge via the Internet at http://pubs.acs.org.

JA031671A